

DYNAMIC ANALYSIS OF ELASTO-INELASTIC FRAMES

by Robert K. Wen^[1] and John G. Janssen^[2]

In this paper a method is presented for the dynamic analysis of plane frames consisting of members having elasto-inelastic bending moment curvature relations. The method is based on a lumped-flexibility and lumped-mass approach in conjunction with a numerical integration procedure for the time dimension. Deformations are assumed to be due to bending only. The procedure of numerical solution is illustrated by an example. Numerical results are presented to show the responses of frames with bilinear moment-curvature relations that range from the perfectly elastic to elasto-perfectly plastic.

Introduction

In recent years the dynamic analysis of elasto-inelastic frames has been discussed by a number of investigators such as DiMaggio (1), Berg and DaDeppo (2), and Heidebrecht, Lee and Fleming (3). All works reported thus far deal with frames having elasto-perfectly plastic moment-curvature relations. The main feature of the method presented in this paper is that it can be used to analyze frames with quite general elasto-inelastic characteristics.

The method of analysis is an extension of a method developed for the dynamic analysis of elasto-inelastic beams by Wen and Toridis (4), and is based on a "lumped flexibility and lumped mass" model to represent the structure and a numerical integration procedure. This of course has the usual advantages of a discretization approach such as the ease in the treatment of discontinuities in the distributions of flexibility and mass, and in the external loading (and/or prescribed foundation movements) in the space and time dimensions.

The use of the method would, in general, require a high speed digital computer. On the other hand, the formulation of the method is based on quite simple and straightforward concepts; its programming for the computer should be a relatively simple task.

The following presentation is limited to plane frames with straight members. Only bending deformation is considered; effects of axial and shear deformations are disregarded. Moreover, the deformations are assumed to be sufficiently small so that their effects on the geometry of the structure are negligible.

^[1],^[2] Associate Professor and Research Assistant, respectively,
Department of Civil Engineering, Michigan State University, U.S.A.

Method of Analysis

Formulation of Model

In order to formulate the model used in the analysis, the first step is to number each member in the frame. Then each member is divided into a number of "panels". It is not necessary to divide all members into the same number of panels. But it is convenient, although not necessary either, to make all panel lengths equal in a given member; and this will be presumed in the subsequent development of the method.

Between the panel points the panels are assumed to be massless and inflexible. The mass and the flexibility of the members are lumped at the panel points on a "tributary" basis, except that the interior joints, at which more than one member meet, are assumed to be rigid.

Shown in Fig. 1b is a typical panel point (i,j) --- the indices i and j refer, respectively, to member i and panel point j. It is emphasized that in this paper indices of this type are generally written inside parentheses rather than as subscripts. The lumped mass at this point is:

$$m(i,j) = \int_{x(i,j) - \frac{1}{2} h(i)}^{x(i,j) + \frac{1}{2} h(i)} m(i,x) dx \quad \dots\dots(1)$$

in which $m(i,x)$ and $h(i)$ are, respectively, the mass distribution and panel length of the i th member. The lumping of the flexibility is effected in the following manner. Let the relation between the bending moment and curvature at point (i,j) for the actual continuous structure be formally represented by the function $g(i,j)$, i.e.,

$$M(i,j) = g(i,j) \text{ [history of curvature at (i,j)]} \quad \dots\dots(2a)$$

Then the relation between the bending moment and the angular deformation at point (i,j), $\theta(i,j)$, may be written as:

$$M(i,j) = f(i,j) \text{ [history of } \theta(i,j)\text{]} \quad \dots\dots(2b)$$

in which $f(i,j) = g(i,j)/h(i)$. (This is tantamount to assuming that the bending moment is constant within the tributary length).

Finally, any lateral loading on a member will also be assumed to be lumped at the panel points.

Equations of Motion

It is convenient to define a "free panel point", or more simply, a "free point", as one which does not coincide with a joint or support and is not immediately adjacent to a joint. For example, points (1,2), (2,5), and (3,3) in Fig.6 are free points. A "constrained panel point" is one that either coincides with a joint (such as points (1,7) and (4,1)) or is immediately adjacent to a joint (such as points (1,6) and (2,2)). A point such as point (1,1) in Fig.6 is a "support point". The equations of motion may be divided into two groups: one for the free points; one for the constrained points.

In Fig.1 are shown the free body diagrams for a typical free point and its two adjacent panels. From Fig. 1b, the equation of motion can be written as:

$$m(i,j) \ddot{y}(i,j) = S^+(i,j) - S^-(i,j) + P(i,j) \quad \dots(3)$$

in which y denotes the transverse displacement. For horizontal members, it is positive downward; for vertical members positive to the right. The dots denote time derivatives, the S 's shears, and the P 's external loads. Referring to Fig.1c and Fig.1d one can express the shears in terms of the moments, and rewrite Eq.2 as:

$$m(i,j) \ddot{y}(i,j) = \frac{1}{h(i)} [M(i,j-1) - 2M(i,j) + M(i,j+1)] + P(i,j) \quad \dots(4)$$

The displacements of the constrained points depend on the rotations of the joints and/or the translations of the floors. In Fig.2 is shown the free body diagram of a typical joint with the associated constrained points. Assuming small rotations, the equation of motion can be written as:

$$J_k \ddot{u}_k = \text{sum of moments about } k \text{ due to the } M\text{'s, } S\text{'s, and the } P\text{'s} \quad \dots(5)$$

in which J_k is the polar moment of inertia about k of the system shown in Fig.2, and u is the angular rotation, positive clockwise. As in the case of Eq.3, the various shears at the constrained points can be expressed in terms of moments via a consideration of the equilibrium of the free body of the adjacent panels. Thus the right-hand side of Eq.5 can be expressed in terms of moments and the external loads only, i.e.,

$$J_k \ddot{u}_k = \text{function of bending moments and external loads} \quad \dots(6)$$

In Fig.3 is shown a free body diagram for a typical floor with all the constrained points associated with the joints of the floor. The equation of motion can be written in the form:

$$m_{fl} \ddot{v}_l = \text{sum of shears (S) and loads (P)} \quad \dots\dots(7)$$

in which m_{fl} is the sum of all the masses shown in Fig.3, and v_l is the horizontal translation of the floor, positive to the right. Likewise, the shears can be expressed in terms of moments via consideration of the equilibrium of the adjacent panels. Thus:

$$m_{fl} \ddot{v}_l = \text{function of bending moments and external loads} \quad \dots\dots(8)$$

Hence, all equations of motion can be expressed in terms of the bending moments and the external loads at the various panel points.

Constraints

The transverse displacements of the constrained points are related to the rotations of the joints, and, in case that such points are in a column, to the horizontal floor displacement also. Under the assumptions that axial deformations are negligible and floor translations are small, the transverse displacements of the end points of any horizontal girder are equal to the vertical component of the ground movement. For two collinear members meeting at a joint, this joint is a panel point to both members. Of course, the transverse displacements of these points are equal. The preceding relations are illustrated by Eqs.22 in a subsequent section on "Numerical Example".

Relation Between Increments of Transverse Displacements and Angular Deformations

From Fig.4, it can be seen that the angular deformation $\theta(i,j)$ is related to the transverse displacements as follows:

$$\theta(i,j) = -\frac{1}{h(i)} [y(i,j-1) - 2y(i,j) + y(i,j+1)] \quad \dots\dots(9)$$

Or, in terms of increments:

$$\Delta\theta(i,j) = -\frac{1}{h(i)} [\Delta y(i,j-1) - 2 \Delta y(i,j) + \Delta y(i,j+1)] \quad \dots\dots(10)$$

The angle is positive, for horizontal members if concave upward; for vertical members concave to the left.

Boundary Conditions

At a hinged or a fixed support, the displacement can be zero or take on prescribed values as in the case of problems involving ground motion.

For a hinged support, the moment is zero. For a fixed support, consider, for example, point (1,1) in Fig.6. The moment $M(1,1)$ depends on the history of $\theta(1,1)$, which is equal to $[y(1,1) - y(1,2)]/h(1)$; the stiffness for this point is twice that of the free points in the same column. The case of the free end of an overhanging girder can be formulated on the basis of zero moment and shear at that end (4).

Bilinear Bending Moment-Curvature or-Rotation Relation

For some elasto-inelastic problems, it is convenient to represent the moment curvature relation by the bilinear type as illustrated in Fig. 5. In the elastic range the stiffness is equal to k_1 ; in the inelastic range the stiffness is k_2 . If a reversal of the direction of the curvature increment takes place while the section is deforming inelastically, the moment curvature relation will return to an elastic path with stiffness k_1 . The total elastic range is assumed to be equal to twice the elastic limit moment M_e .

For the lumped flexibility model, one deals with rotation instead of curvature. To facilitate the computation of the increment of bending moment ΔM corresponding to a given $\Delta\theta$, it is convenient to introduce the quantities: "positive and negative transition moments", N^+ and N^- , which are defined to be respectively, the magnitudes of the changes in moment that would just initiate inelastic behavior in the positive and negative direction (see Fig.5). At the virgin state, $M = 0$, and both N^+ and N^- are equal to M_e . It is noted that at all times $N^+ + N^- = 2 M_e$.

The use of the transition moments in computing the moment increments is illustrated in the following. (The transition moments may be regarded as representing the influence of the "past history" of the angular deformation). Referring to Fig.5, the problem may be stated as: given

$M(t)$, $N^+(t)$, $N^-(t)$ and $\Delta\theta = \theta(t + \Delta t) - \theta(t)$, it is required to find

$$\Delta M = M(t + \Delta t) - M(t)$$

If $\Delta\theta$ is positive or zero, but less than $N^+(t)/k_1$:

$$\Delta M = k_1 \Delta\theta$$

$$N^+(t + \Delta t) = N^+(t) - \Delta M \quad \} \dots\dots(11a-c)$$

$$N^-(t + \Delta t) = 2M_e - N^+(t + \Delta t)$$

If $\Delta\theta$ is positive or zero, and larger than or equal to $N^+(t)/k_1$:

$$\Delta M = N^+(t) + k_2 [\Delta\theta - N^+(t)/k_1]$$

$$\begin{aligned}
 N^+(t + \Delta t) &= 0 \\
 N^-(t + \Delta t) &= 2 M_e \quad \dots\dots(12a-c)
 \end{aligned}$$

If $\Delta\theta$ is negative or zero, but algebraically larger than or equal to $(-N^-(t)/k_1)$:

$$\begin{aligned}
 \Delta M &= k_1 \Delta\theta \\
 N^-(t + \Delta t) &= N^-(t) - \Delta M \\
 N^+(t + \Delta t) &= 2 M_e - N^-(t + \Delta t) \quad \dots\dots(13a-c)
 \end{aligned}$$

If $\Delta\theta$ is negative, and algebraically less than $(-N^-(t)/k_1)$:

$$\begin{aligned}
 \Delta M &= -N^-(t) + k_2 [\Delta\theta + N^-(t)/k_1] \\
 N^-(t + \Delta t) &= 0 \\
 N^+(t + \Delta t) &= 2 M_e \quad \dots\dots(14a-c)
 \end{aligned}$$

Of course, $N^+(t + \Delta t)$ and $N^-(t + \Delta t)$ are computed for use in the next time interval in the numerical solution.

Summary of Procedure of Analysis

Let Y be a column matrix containing the transverse displacements for all the panel points in the frame. From previous discussions, the matrix Y may be considered to be made of three sub-matrices, i.e., $Y = \{Y_1 \ Y_2 \ Y_3\}$, in which Y_1 contains the displacements of the previously defined free points, Y_2 contains those displacements defined by constraints, and Y_3 contains the prescribed boundary or support points. Also from previous discussions, there are three sets of equations of motion:

$$\begin{aligned}
 \bar{m} \ddot{Y}_1 &= A_1 \bar{M} + B_1 \bar{P} \\
 \bar{J} \ddot{U} &= A_2 \bar{M} + B_2 \bar{P} \\
 \bar{m}_f \ddot{V} &= A_3 \bar{M} + B_3 \bar{P} \quad \dots\dots(15a-c)
 \end{aligned}$$

in which \bar{m} is the mass matrix for the free points, \bar{J} is the matrix of the polar moments of inertia of the joints, \bar{m}_f is the mass matrix of the

floors, U is the acceleration matrix of the joint rotations, V is the matrix of the horizontal accelerations of the floors, \bar{M} and \bar{P} are matrices for bending moments and loads, respectively, and A_1, \dots, B_3 are matrices of appropriate sizes containing constants whose values depend only on the panel lengths of the members.

The displacements defined by constraints can be written as:

$$Y_2 = C_1 U + C_2 V \quad \dots(16)$$

in which C_1 and C_2 are matrices with known elements.

The problem of numerical solution may be stated as follows: Given at time t , $Y(t)$, $U(t)$, $V(t)$, and $\bar{M}(t)$, it is required to determine, for time $t + \Delta t$, the transverse displacements, the deformations and bending moments of the panel points. The procedure of solution may be outlined as follows:

(1) From Eqs.15, compute the accelerations at t .

(2) Having obtained the accelerations at t , use some type of numerical integration procedure to obtain the changes in velocities and displacements for the interval Δt . A procedure for this purpose is for example, described in Reference (5). In this manner, ΔY_1 , ΔU , ΔV are obtained. From Eq.16, obtain ΔY_2 . Since ΔY_3 are prescribed, ΔY is completely known.

(3) From ΔY , the incremental angular deformations of the various panel points can be computed from the relationship as given by Eq.10.

(4) From the changes in angular deformation the corresponding changes in bending moment can be computed from prescribed bending moment-rotation relations, such as represented by Eqs.11 - 14.

(5) Setting $Y(t + \Delta t) = Y(t) + \Delta Y$; $U(t + \Delta t) = U(t) + \Delta U$, $V(t + \Delta t) = V(t) + \Delta V$, and $\bar{M}(t + \Delta t) = \bar{M} + \Delta \bar{M}$, the solution can be carried on to the next time instant $t + 2 \Delta t$ by repeating the steps (1) through (4), and so on.

Numerical Example

The structure considered is a two-story symmetrical frame shown in Fig.6, subjected to a horizontal ground motion as depicted in Fig.7. The frame is initially at rest. The properties of the members are listed in Table 1. Within each member the stiffness and mass distributions are uniform. On account of symmetry only one half of the structure need be considered. The columns are divided into six equal panels, and the girders twelve. The panel lengths are thus equal for all members.

The free points in the frame are: (1,2), (1,3), (1,4), (1,5); (2,3), (2,4), (2,5); (3,3), (3,4), (3,5), (3,6); (4,3), (4,4), (4,5), (4,6); -- a total of 15. The constrained points are: (1,6), (2,2), (3,2); (1,7), (2,1), (3,1); (4,2), (2,6); (4,1), (2,7); -- a total of 10. The boundary or support points are: (1,1), (3,7), (4,7) -- a total of 3. Thus there are 28 points -- each member with 7.

For each of the free points there is an equation of motion similar to Eq.4:

$$m(i) h(i) \ddot{y}(i,j) = \frac{1}{h(i)} [M(i,j-1) - 2 M(i,j) + M(i,j+1)] \quad \dots\dots(17)$$

in which $m(i)$ is the mass per unit length of the i th member. The equations of motion for the rotations of the joints at the first and second floors are, respectively:

$$J(i)\ddot{u}(1) = 2 [M(1,6) - M(2,2) - M(3,2)] + M(2,3) - M(1,5) + M(3,3) \quad \dots\dots(18)$$

$$J(2)\ddot{u}(2) = 2 [M(2,6) - M(4,2)] + M(4,3) - M(2,5) \quad \dots\dots(19)$$

in which $J(1) = m(1) h(1)^3 + m(2) h(2)^3 + m(3) h(3)^3$, and

$$J(2) = m(2) h(2)^3 + m(4) h(4)^3.$$

The equations of motion for the translations of the first and second floors are, respectively:

$$m_{1f} \ddot{v}(1) = \frac{1}{h(2)} [M(2,3) - M(2,2)] + \frac{1}{h(1)} [M(1,5) - M(1,6)] \quad \dots\dots(20)$$

$$m_{2f} \ddot{v}(2) = \frac{1}{h(2)} [M(2,5) - M(2,6)] \quad \dots\dots(21)$$

in which $m_{1f} = 1.5 [m(1) h(1) + m(2) h(2)] + 6 h(3) m(3)$, and

$$m_{2f} = 1.5 m(2) h(2) + 6 h(4) m(4).$$

The displacements of the constrained points are computed as follows:

$$y(3,2) = h(3) u(1) ; \quad y(1,7) = v(1) ; \quad y(2,1) = v(1)$$

$$\begin{aligned}
y(2,7) &= v(2) & ; & & y(4,1) &= 0 & ; & & y(3,1) &= 0 \\
y(2,2) &= v(1) + h(2) u(1) & ; & & y(1,6) &= v(1) - h(1) u(1) & \} & \dots\dots & (22) \\
y(2,6) &= v(2) - h(2) u(2) & ; & & y(4,2) &= h(4) u(2)
\end{aligned}$$

The displacements at the support points are:

$$y(3,7) = 0 \quad ; \quad y(4,7) = 0 \quad \dots\dots(23ab)$$

$$y(1,1) = \text{function graphed in Fig. 7} \quad \dots\dots(24)$$

Combining Eqs. 17, 22, 23, and 24, one has 28 equations for the 28 displacements. These displacements are sufficient to compute all the angular deformations needed, which in turn, yields the bending moments. Note that $M(3,7) = M(4,7) = 0$, and the bending moments at the joints are not needed in the analysis. The moment-rotation relations are assumed to be the bilinear type as described previously. The value of k_1 for each panel point is equal to the bending rigidity divided by the panel length. The ratio $R = k_2/k_1$ is considered as a parameter.

For the numerical integration the following formulas (5) were used:

$$\begin{aligned}
\Delta z &= \Delta t \dot{z}(t) + \frac{1}{2} (\Delta t)^2 \ddot{z}(t) \\
\Delta \dot{z} &= \frac{1}{2} \Delta t [\ddot{z}(t) + \ddot{z}(t + \Delta t)]
\end{aligned}
\quad \dots\dots(25ab)$$

in which z denotes any of the displacement unknowns, and the prefix Δ denotes change from t to $(t + \Delta t)$. The size of Δt used was 1.055×10^{-4} seconds.

The response of the frame was considered for eight values of the ratio R , ranging from zero (elasto-perfectly plastic case) to unity (perfectly elastic case). The quantities computed are, for each panel point, the maximum positive angular deformation $\theta_{p,max}$, and the absolute value of the maximum negative angular deformation $\theta_{n,max}$. In Table 2 are listed, for $R = 0, 0.2, \text{ and } 1.0$, these quantities scaled by the respective "yield angle" θ_e (see Fig. 5), i.e., $\bar{\theta}_{p,max} = \theta_{p,max} / \theta_e$; and $\bar{\theta}_{n,max} = \theta_{n,max} / \theta_e$. Listed also are the values of t_p and t_n which denote the times (in seconds) at which these maximum deformations occur.

It may be seen from these tables that only at four points: (1,1), (1,2), (1,6), and (2,2), the deformations have gone into the inelastic range as signified by the fact that the value of $\bar{\theta}_{p,max}$ or $\bar{\theta}_{n,max}$ has exceeded unity.

In Figs. 8, 9, and 10 are shown the influence of the ratio R on the response for these four points. The values of $\bar{\theta}_{p,max}$ are plotted in Fig. 8. It is seen that the values of $\bar{\theta}_{p,max}$ for point (1,1) and point (1,2) vary considerably with R . While at (1,1) the deformation decreases with R , at (1,2) it increases with R . The rate of changes is largest in the neighborhood of $R = 0.2$ and levels off at approximately $R = 0.6$. For points (1,6) and (2,2) the values of $\bar{\theta}_{p,max}$ increase slightly with R .

Graphs of $\bar{\theta}_{n,max}$ are shown in Fig. 9. For point (1,1), the deformation increases with R for $R < 0.2$; and decreases with R for $R > 0.2$. The opposite is true for point (1,2). For points (1,6) and (2,2), the influence of R is small.

In Fig. 10 are plotted the "ranges of inelastic deformation", i.e., $\bar{\theta}_{p,max} + \bar{\theta}_{n,max}$. It is seen that for $R < 0.4$, point (1,1) has the greatest range of inelastic deformation; and for $R > 0.4$, point (1,6) has. The results presented in the preceding would seem to indicate that the parameter R could have a significant influence on the mode of deformation of the structure.

Concluding Remarks

It is obvious that the method described here can be applied to structures with other elasto-inelastic properties, such as the elasto-perfectly plastic and then strain-hardening type as for the structural mild steel. Effects of damping and strain rate can be incorporated in the analysis. The influence of dead and live loads can also be taken into account by setting the bending moments to appropriate initial values. Moreover, the static behavior of frames with general inelastic properties can also be treated by the method as a quasi dynamic problem as, for the elasto-perfectly plastic case, suggested by Newmark (5) and recently demonstrated by Heidebrecht, Lee, and Fleming (3).

The accuracy of the method apparently depends on the numbers of panels into which the various members of the frame are divided. As mentioned before, it is not necessary that all members be divided into the same number of panels. For example, if the critical members of a study are the columns, they can be divided into more panels than the floor girders. Intuitively, it is reasonable to expect that, as the numbers of panels increase, the solution would converge to the case of continuous distributions of flexibility and mass. This, indeed, seems to be the case for a simple beam (4). However, the amount of computation, and hence the computer time needed to cover a given range of integration in the time dimension, increases at a high rate (approximately at third power) with the total number of "free panel points" in the frame. This in general imposes a practical limit on the number of panel points that can be used for a given computer. Furthermore, with increasing amount of computation the round-off error grows rapidly. This also must be taken into

account in the choice of the numbers of panels.

Acknowledgment

Gratitude is extended to National Science Foundation for their support of this work under Grant No. 12143.

References

1. DiMaggio, F. L., "Dynamic Elasto-plastic Response of Rigid Frames", Journal of Engineering Mechanics, ASCE, Vol. 84, EM3, July 1958.
2. Berg, G. V., and DaDeppo, D. A., "Dynamic Analysis of Elasto-Plastic Structures", Journal of Engineering Mechanics, ASCE, Vol. 86, EM2, April 1960.
3. Heidebrecht, A., Lee, S., and Fleming, J., "Dynamic Analysis of Elasto-plastic Frames", Journal of the Structural Division, ASCE, Vol. 90, ST2, April 1964.
4. Wen, R., and Toridis, T., "Discrete Dynamic Models for Elasto-Inelastic Beams", Progress Report No.2, NSF Project G12143, Division of Engineering Research, Michigan State University, March 1964.
5. Newmark, N. M., "A Method of Computation for Structural Dynamics", Trans. ASCE, Vol. 127, 1962, p.1406.

TABLE 1. Properties of Frame

Member	i = 1, or 2	i = 3	i = 4
Length (ft)	12	24	24
Weight per unit length (lb/ft)	31	1000	500
Bending Rigidity (lb-in ²)	3.29×10^9	10.18×10^9	4.72×10^9
Elastic Limit Moment (in-lb)	822.8×10^3	1453.7×10^3	943.8×10^3

TABLE 2-a Maximum Deformations

R = 0.0

i		j = 1	j = 2	j = 3	j = 4	j = 5	j = 6
1	$\bar{\theta}_{p,max.}$	6.048	0.851	0.635	0.391	0.759	1.102
	t_p	0.055	0.050	0.051	0.059	0.083	0.102
	$\bar{\theta}_{n,max.}$	-2.141	-0.850	-0.621	-0.444	-0.691	-2.774
	t_n	0.254	0.073	0.069	0.063	0.041	0.052
2	$\bar{\theta}_{p,max.}$	0.000	1.066	0.656	0.349	0.347	0.787
	t_p	0.000	0.080	0.082	0.254	0.162	0.159
	$\bar{\theta}_{n,max.}$	0.000	-1.450	-0.625	-0.219	-0.237	-0.543
	t_n	0.000	0.162	0.159	0.034	0.429	0.431
3	$\bar{\theta}_{p,max.}$	0.000	0.395	0.341	0.351	0.230	0.234
	t_p	0.000	0.148	0.141	0.144	0.138	0.191
	$\bar{\theta}_{n,max.}$	0.000	-0.465	-0.413	-0.396	-0.290	-0.206
	t_n	0.000	0.041	0.043	0.036	0.035	0.032
4	$\bar{\theta}_{p,max.}$	0.000	0.799	0.704	0.572	0.426	0.263
	t_p	0.000	0.167	0.169	0.163	0.160	0.158
	$\bar{\theta}_{n,max.}$	0.000	-0.643	-0.561	-0.573	-0.369	-0.304
	t_n	0.000	0.415	0.410	0.411	0.407	0.416

TABLE 2-b,c Maximum Deformations

R = 0.2

i		j = 1	j = 2	j = 3	j = 4	j = 5	j = 6
1	$\bar{\theta}_{p,max.}$	3.638	2.072	0.825	0.508	0.811	1.535
	t_p	0.047	0.051	0.051	0.058	0.083	0.102
	$\bar{\theta}_{n,max.}$	-3.265	-0.116	-0.694	-0.499	-0.673	-3.102
	t_n	0.105	0.001	0.101	0.138	0.020	0.052
2	$\bar{\theta}_{p,max.}$	0.000	1.297	0.678	0.359	0.376	0.810
	t_p	0.000	0.089	3.916	0.246	0.180	0.177
	$\bar{\theta}_n$	0.000	-1.656	-0.639	-0.229	-0.258	-0.586
	t_n	0.000	0.174	0.150	0.034	0.052	0.089
3	$\bar{\theta}_{p,max.}$	0.000	0.422	0.363	0.389	0.250	0.242
	t_p	0.000	0.148	0.142	0.144	0.145	0.191
	$\bar{\theta}_{n,max.}$	0.000	-0.496	-0.438	-0.419	-0.302	-0.235
	t_n	0.000	0.041	0.043	0.036	0.035	0.061
4	$\bar{\theta}_{p,max.}$	0.000	0.900	0.696	0.599	0.432	0.279
	t_p	0.000	0.169	0.164	0.164	0.160	0.159
	$\bar{\theta}_{n,max.}$	0.000	-0.694	-0.612	-0.605	-0.394	-0.323
	t_n	0.000	0.076	0.079	0.080	0.082	0.084
R = 1.0							
1	$\bar{\theta}_{p,max.}$	1.605	3.348	0.806	0.534	0.696	1.756
	t_p	0.022	0.051	0.051	0.073	0.079	0.102
	$\bar{\theta}_{n,max.}$	-1.838	-0.896	-0.729	-0.541	-0.648	-3.370
	t_n	0.081	0.101	0.076	0.138	0.020	0.052
2	$\bar{\theta}_{p,max.}$	0.000	1.370	0.703	0.355	0.391	0.828
	t_p	0.000	0.082	0.074	0.245	0.183	0.159
	$\bar{\theta}_{n,max.}$	0.000	-1.789	-0.657	-0.229	-0.265	-0.585
	t_n	0.000	0.168	0.152	0.152	0.052	0.089
3	$\bar{\theta}_{p,max.}$	0.000	0.429	0.406	0.425	0.304	0.253
	t_p	0.000	0.148	0.141	0.144	0.138	0.147
	$\bar{\theta}_{n,max.}$	0.000	-0.490	-0.440	-0.415	-0.306	-0.279
	t_n	0.000	0.047	0.043	0.036	0.035	0.062
4	$\bar{\theta}_{p,max.}$	0.000	0.984	0.721	0.612	0.444	0.302
	t_p	0.000	0.172	0.169	0.166	0.161	0.162
	$\bar{\theta}_{n,max.}$	0.000	-0.703	-0.614	-0.622	-0.410	-0.325
	t_n	0.000	0.076	0.079	0.080	0.081	0.084

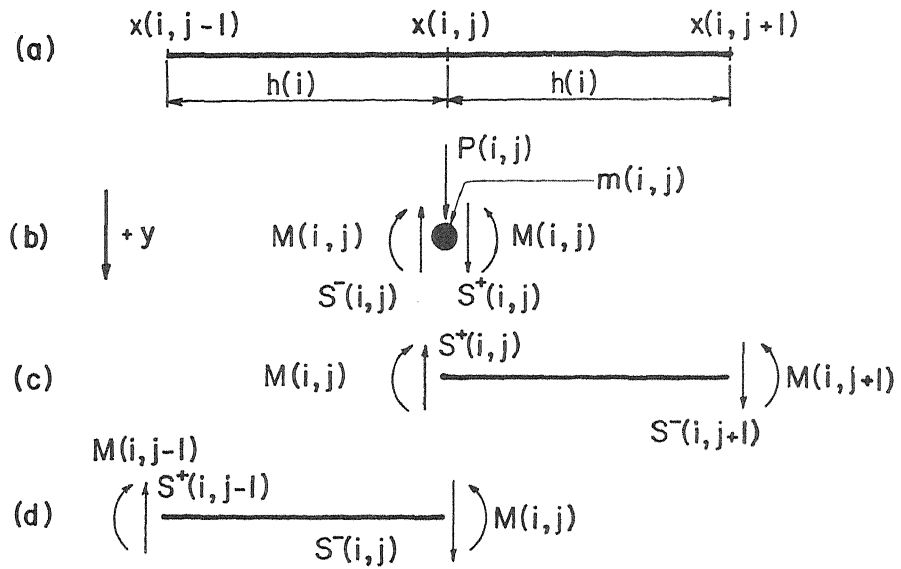


FIG. 1. FREE BODY DIAGRAMS FOR TYPICAL PANELS

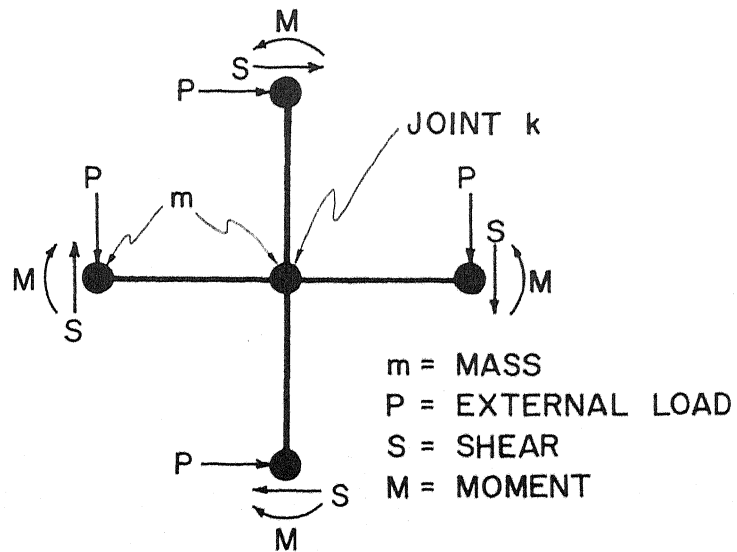
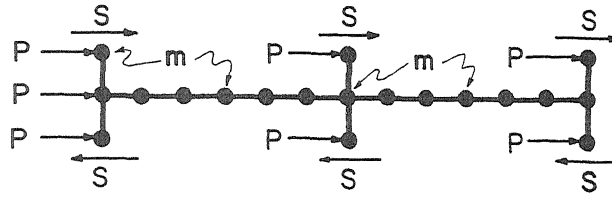


FIG. 2. FREE BODY OF TYPICAL JOINT



P = EXTERNAL LOADS
 S = SHEARS
 m = MASSES

FIG. 3. FREE BODY DIAGRAM FOR CONSIDERING HORIZONTAL TRANSLATION OF TYPICAL FLOOR

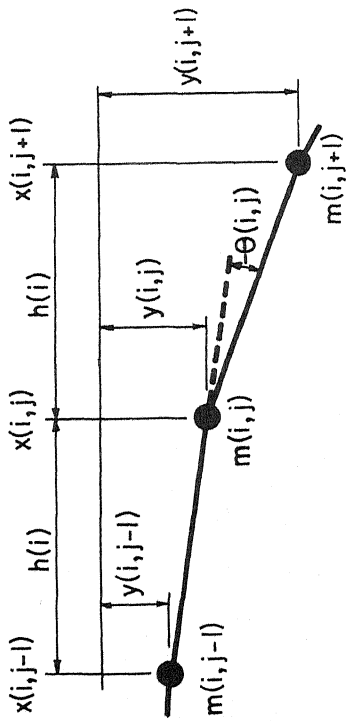


FIG. 4. RELATION BETWEEN y AND θ .

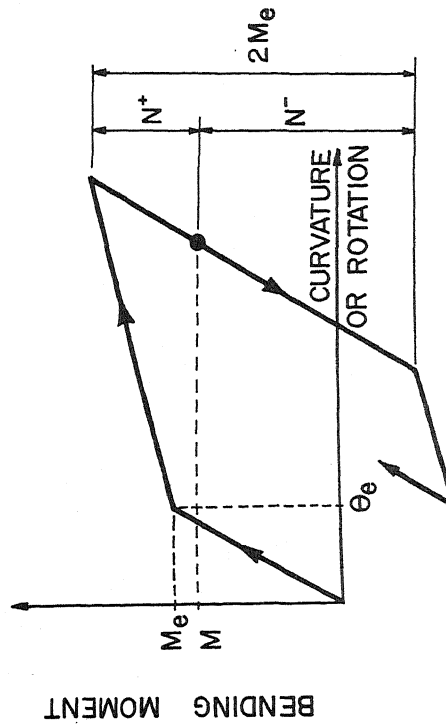


FIG. 5. BILINEAR BENDING MOMENT - CURVATURE (OR ROTATION) RELATION

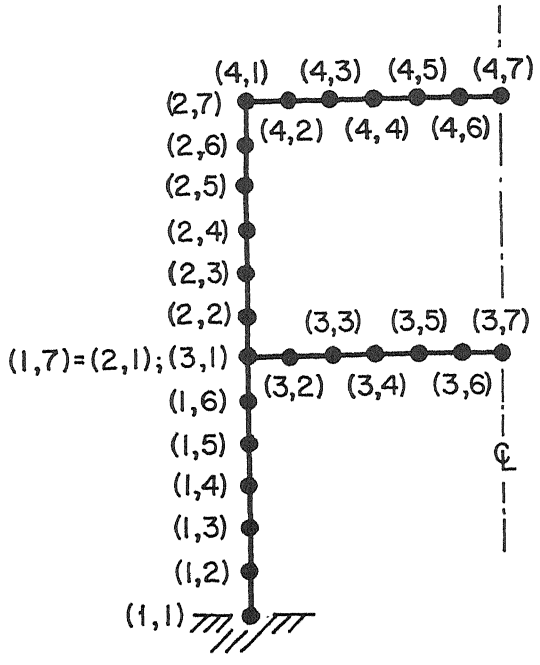


FIG. 6. TWO STORY FRAME

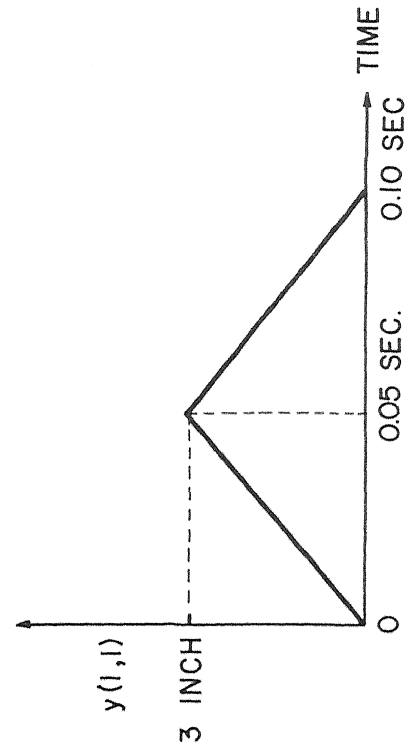


FIG. 7. HORIZONTAL GROUND MOTION (PRESCRIBED $y(1,1)$)

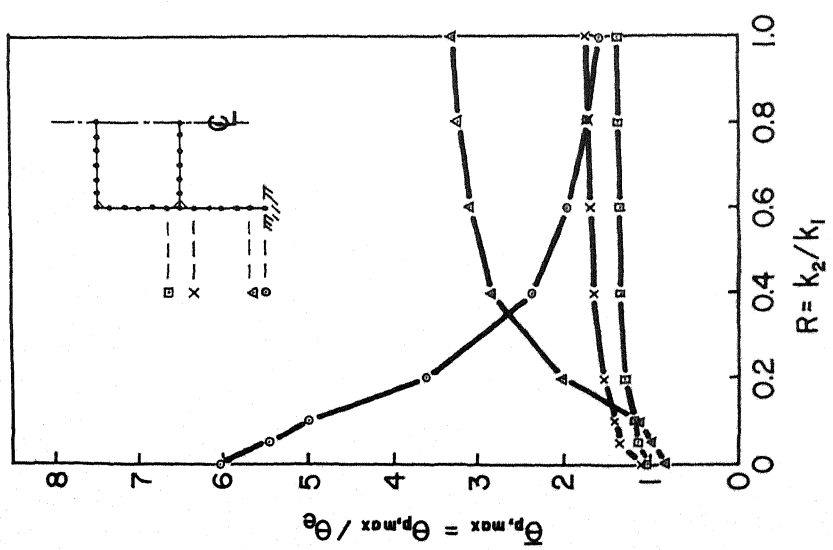


FIG. 8. EFFECT OF R ON $\bar{\theta}_{p,max}$

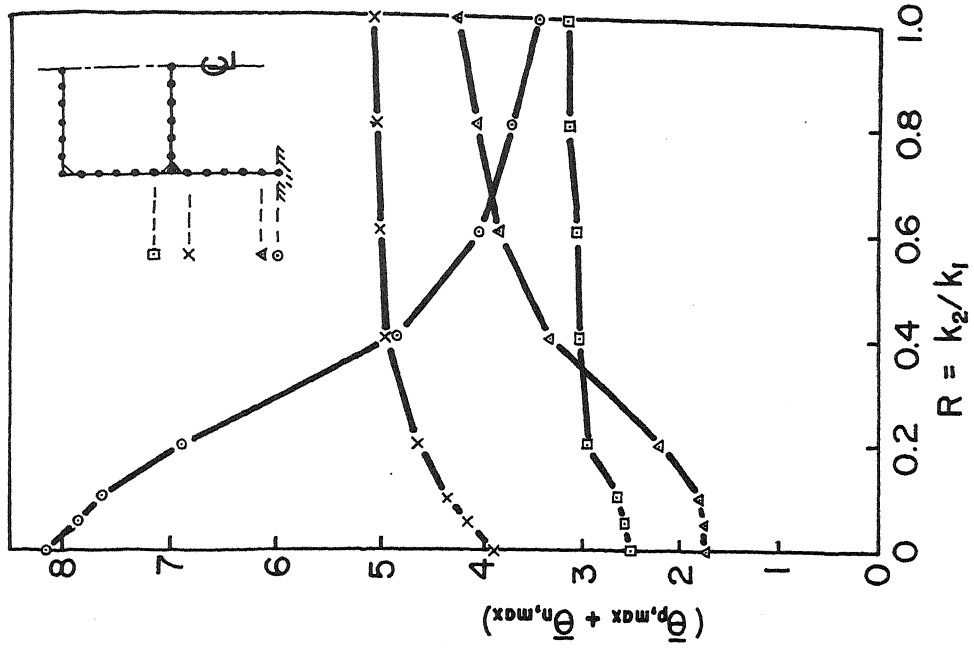


FIG. 10. EFFECT OF R ON RANGE OF DEFORMATION

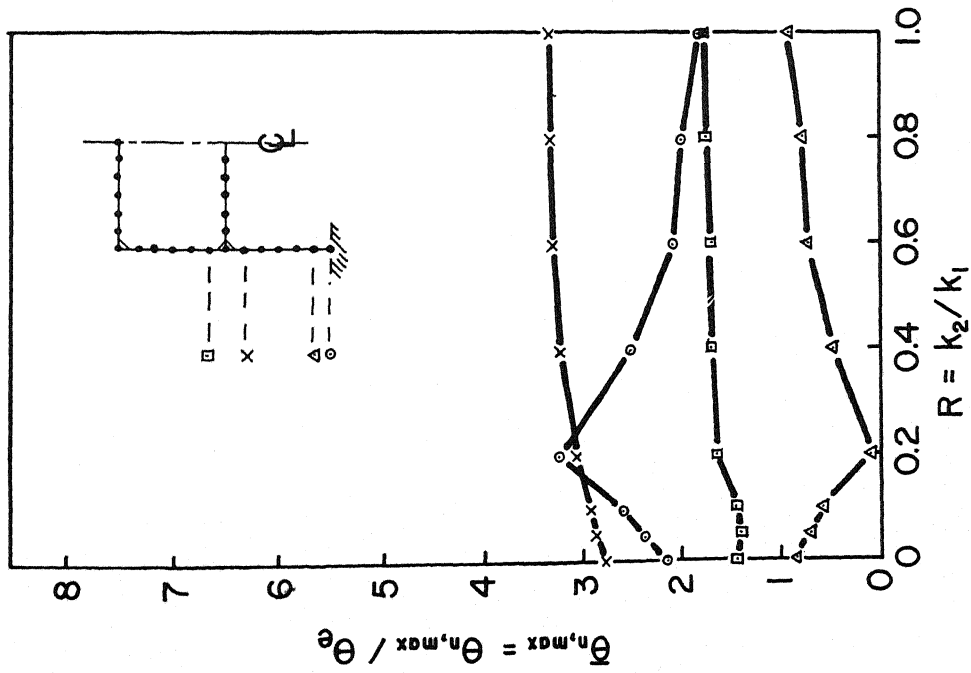


FIG. 9. EFFECT OF R ON $\bar{\theta}_{n,max}$